

## Pb(II) removal from aqueous solution by cold KOH activated biochar of camphor leaves: isotherms, kinetics and thermodynamics

Cui Li<sup>a,b</sup>, Hui Wang<sup>a,\*</sup>, Yingshuang Zhang<sup>a,\*</sup>

<sup>a</sup>*School of Chemistry and Chemical Engineering, Central South University, Changsha, 410083 Hunan, China, Tel. +0731-88879616/+86 13973138633; email: huiwang1968@163.com (H. Wang), Tel. +18040039219; email: 18742487986@163.com (Y. Zhang), Tel. +86 13808781881; email: Lc9\_11982@163.com (C. Li)*

<sup>b</sup>*Dehong Teachers' College, Mangshi 678400, Yunnan, China*

Received 6 November 2018; Accepted 19 April 2019

### ABSTRACT

Biochar from camphor leaves was activated by low-cost cold KOH process (ABC) to improve Pb(II) removal from aqueous solution. Then ABC was characterized by Fourier transform infrared spectroscopy, X-ray diffraction, scanning electron microscopy and N<sub>2</sub> adsorption–desorption to reveal the benefits of cold KOH activation. The high adsorption capacity of ABC mainly results from oxygen-containing groups, porous structure and large surface area. Effect of factors including dose of ABC, pH, ionic strength, adsorption time, and temperature on Pb(II) adsorption was investigated by monofactor experiments. Through comparison with biochar (BC), optimization of ABC adsorption was revealed by kinetics, isotherms and thermodynamics. Pb(II) adsorption onto ABC is well described by pseudo-second-order kinetics and Langmuir isotherm, implying that chemisorption and monolayer adsorption are the rate-limiting steps. The thermodynamics indicates that Pb(II) adsorption onto ABC is spontaneous and exothermic. After cold KOH activation, the maximum adsorption capacity of Pb(II) onto ABC is 90.09 mg g<sup>-1</sup>, higher than 62.27 mg g<sup>-1</sup> of BC. ABC has an excellent dynamic and thermodynamic performance comparing with BC.

*Keywords:* Adsorption; Biochar; KOH activation; Lead removal; Wastewater

### 1. Introduction

Pollution of heavy metals has been a serious environmental problem in developing countries, since heavy metals are toxic, bioaccumulative and non-biodegradable [1]. Heavy metals include lead, cadmium, mercury, chromium, arsenic and so on, posing considerable threat to animals and human beings [2]. Lead is one of the most toxic heavy metals for water pollution, and its accumulation in tissues can have harmful physiological effects [3]. China faces serious lead pollution in the past decades. People living in Guazhou city, Dafeng city, Longchang city and Jiahe city, suffered from elevated blood lead levels [4]. Moreover, approximately

23.9% of Chinese children were subjected to a blood lead level higher than 100 µg L<sup>-1</sup> [5]. Therefore, removing heavy metals, especially lead, from wastewater is an imperative process in China.

Numerous methods were proposed for removing heavy metals from aqueous solution, such as chemical precipitation, electrochemical treatment, reverse osmosis, ion exchange and membrane separation [6,7]. For examples, the titanate nanomaterials of flaky structure were synthesized at 130°C for about 24 h to get a high adsorption capacity of 504.12 mg g<sup>-1</sup>, resulting from the chemical precipitation with adequate hydroxyl groups [8]. Composite membrane with cellulose and graphene oxide was prepared by phase

\* Corresponding authors.

inversion to remove the heavy metal from aqueous solution, achieving 100% removal of lead, zinc and nickel [9]. Silicate-based ion-exchange resin compromised by activated non-metallic fraction of printed circuit board was used to adsorb lead ions and research the equilibrium saturation-exchange capacities [10]. These techniques are limited for commercial application due to high cost, complex operation and generating wastes. Adsorption is promising for removing heavy metals and receiving increasing worldwide attention [11,12].

In the past decade, biochar gained great attention due to unique properties and promising applications [13,14]. Because of large surface area and abundant functional groups, biochar is a promising adsorbent for removing heavy metals. Various wastes, including sesame straw [15], marine macro-algal [16], rice straw [17], sugar cane bagasse and orange peel [18], were used to prepare biochar for adsorption of heavy metals. In general, biochar has limited adsorption capacity, and surface modifications can improve adsorption performance of biochar for removing heavy metals, such as chemical modification and nano-particle loading. Pi et al. [19] modified biochar with  $C_3N_4$  nano-particles as an adsorptive and photocatalytic material for decontamination of aqueous solution. In addition, EDTA [20],  $MnO_x$  nano-particles [21] and magnetic particles [22] were also applied to modify biochar and enhance the adsorption capacity of it. Wang et al. [7] functionalized biochar using succinic anhydride to enhance the adsorption capacity via increasing the amount of carboxyl groups [7]. Aian et al. [23] sulfur-functionalized bamboo powder by mercaptoacetic acid and successfully improved the adsorption capacity of biochar. Most proposed modifications suffer from complex operation and high cost. Simple, cheap and effective modification of biochar is necessary to improve heavy metal adsorption.

Previous studies reported that cold potassium hydroxide activation of hydrochar was effective to enhance adsorption of heavy metals [24,25]. Cold potassium hydroxide activation is a promising modification for commercial application owing to low cost and easy operation. To the best of our knowledge, there is little work about cold KOH activation of biochar for removing heavy metals. Pb(II) was chosen as target heavy metal in this work. Local waste as raw material for biochar preparation is favorable for solving Pb(II) pollution in China. Locally available fallen leaves were used to prepare biochar, and cold KOH activation was conducted to improve Pb(II) adsorption. Biochar activated by cold KOH solution was characterized by Fourier transform infrared spectroscopy (FTIR), X-ray diffraction (XRD), scanning electron microscopy (SEM) and  $N_2$  adsorption-desorption. Effect of ABC dose, pH, adsorption time, initial concentration, ionic strength and temperature was investigated. Adsorption kinetics, isotherms and thermodynamics were conducted to reveal adsorption mechanism.

## 2. Materials and methods

### 2.1. Materials

Fallen leaves of camphor tree were used as raw materials for preparation of biochar, and they were obtained from Yuelu Mountain, Changsha, China. The fallen leaves were washed

with distilled water three times to remove the remaining dust, dried at 80°C for 10 h in a vacuum oven (DZF6032, Jiangsu Kangjin Instrument Co. Ltd., China), crushed using a plant grinder (FW-177, Tianjin Taisite Instrument Co. Ltd., China), and screened into 0.075–0.15 mm with standard sieves. Lead nitrate, potassium hydroxide, nitric acid, sodium chloride and calcium chloride were of analytical reagent grade, purchased from Sinopharm Chemical Reagent Co. Ltd., China and used without further purification.

### 2.2. Biochar preparation

The pretreated fallen leaves (3 g) were put into a 30 mL ceramic crucible with lid. Then, the ceramic crucible was put in a muffle furnace at 450°C for 2 h. After cooling to room temperature, the obtained material was referred as biochar (BC). The biochar was mixed with 100 mL of 1 mol L<sup>-1</sup> KOH solution in 200 mL of conical flask, and then stirred for 60 min at 30°C with a stirring rate of 300 rpm. After activation, the biochar was sufficiently washed with distilled water until neutral pH was reached, the biochar referred as ABC was obtained after vacuum filtration and drying at 100°C for 10 h.

### 2.3. Characterizations

FTIR spectrum was recorded using a Nicolet Avatar 360 Fourier transform infrared spectroscopy (PerkinElmer Inc., USA). XRD pattern was examined by a D-500 X-ray diffractometer (Siemens Corp., Belgium) with Cu K $\alpha$  radiation. SEM was performed using a Nova NanoSEM 230 scanning electron microscopy (FEI, USA).  $N_2$  adsorption-desorption was conducted via an Autosorb-1 gas analyzer (Quantachrome, USA) to determine the specific surface area. Small amount of ABC was added in 50 mL deionized water and ultrasonicated for 10 min. The obtained suspension was used to measure the pH of zero charge via potential meter (NanoBrook 90plus, Brookhaven, United States). 0.1 mol L<sup>-1</sup> nitric chloride and sodium hydroxide were used to adjust pH value of this suspension liquid.

### 2.4. Batch adsorption

Standard solution with 1 g L<sup>-1</sup> Pb(II) was prepared by dissolving 1.6000 g lead nitrate into 1 L distilled water. Serial Pb(II) solution with different Pb(II) concentration was prepared by diluting the standard solution. Certain dosage of BC or ABC was put into a 150 mL conical flask with 25 mL diluted Pb(II) solution, and adsorption was conducted in a thermostatic oscillator at 25°C at a speed of 200 rpm. Effect of dosage (0.04–0.14 g), solution pH (1.0–6.0), contact time (1–60 min for ABC and 1–360 min for BC) and temperature (25°C–45°C) was investigated by batch adsorption tests. The initial pH of lead ions solution was adjusted by 0.1–1.0 mol L<sup>-1</sup> nitric acid. Pb(II) concentration in aqueous solution was determined using an Optima 5300 DV inductively coupled plasma spectrometry (ICP, PerkinElmer, USA). The parameters selected in certain adsorption experiment were detailed in figure captions. Pb(II) removal and adsorption capacity were calculated by Eqs. (1) and (2). Adsorption kinetics, isotherms and thermodynamics were

conducted in 25 mL Pb(II) solution at a speed of 200 rpm and studied using Eqs. (3)–(8). To investigate the effect of ionic strength on Pb(II) adsorption on ABC, 0.02–0.1 mol L<sup>-1</sup> of NaCl and CaCl<sub>2</sub> was added to 200 mg L<sup>-1</sup> solution of 25 mL at pH 6.0.

$$R = \frac{(C_0 - C)}{C_0} \quad (1)$$

$$Q = (C_0 - C) \times \frac{V}{m} \quad (2)$$

$$\ln(Q_e - Q) = \ln Q_e - k_1 \times t \quad (3)$$

$$\frac{t}{Q} = \frac{1}{(k_2 \times Q_e^2)} + \frac{t}{Q_e} \quad (4)$$

$$\frac{C_e}{Q_e} = \frac{1}{(b \times Q_m)} + \frac{C_e}{Q_m} \quad (5)$$

$$\log Q_e = \log k_f + \frac{1}{n} \times \log C_e \quad (6)$$

$$\ln K = \frac{\Delta S}{R} - \frac{\Delta H}{(R \times T)} \quad (7)$$

$$\Delta G = -RT \times \ln K \quad (8)$$

where  $R$  is the removal ratio of Pb(II);  $C_0$  and  $C$  are the Pb(II) concentration before and after adsorption, respectively;  $V$  is the volume of Pb(II) solution;  $m$  is the mass of ABC;  $t$  is the adsorption time;  $Q$ ,  $Q_e$  and  $Q_m$  are the adsorption capacity, equilibrium capacity and maximum capacity, respectively;  $k_1$  and  $k_2$  are the rate constants of pseudo-first-order and pseudo-second-order kinetic models;  $b$  is the Langmuir parameter;  $n$  and  $k_f$  are Freundlich parameters;  $K$  is the equilibrium constant;  $T$  is the thermodynamic temperature;  $R$  is the gas constant;  $\Delta G$ ,  $\Delta S$  and  $\Delta H$  is the Gibbs free energy, entropy change and enthalpy change, respectively.

### 2.5. Regeneration of adsorbent

Adsorption and desorption experiments were conducted four times to investigate the reusability of adsorbent. The initial concentration of lead ion solution was 200 mg L<sup>-1</sup> that was constant in the adsorption/desorption cycles. Modified adsorbent (ABC) was shook in 200 mL conical flask with biochar dosage 4 g L<sup>-1</sup>, adsorption time 30 min, pH 6.0 and temperature 25°C. Then these adsorbents were immersed and shook in 25 mL HCl (0.2 mol L<sup>-1</sup>) for 30 min to desorb lead ions. The same adsorbent was used in every cycle after careful elution by de-ionized water for several times to remove any traces of acid. Regeneration of adsorbent was evaluated by adsorption capacity of Pb(II).

## 3. Results and discussion

### 3.1. Biochar characterization

Fig. 1a shows the FTIR spectrum of ABC. The broad strong peak at 3,200–3,600 cm<sup>-1</sup> is assigned to hydroxyl groups. The peaks at 2,930 and 2,860 cm<sup>-1</sup> are attributed to symmetric and asymmetric vibration of aliphatic -CH<sub>2</sub>, and the weak peaks indirectly verify aromatic structure of ABC. The peak at 1,400 cm<sup>-1</sup> attributed to C=C bond also indicates the aromatic structure of ABC. Oxygenic functional groups are verified by the peaks at 1,620; 1,170; 1,090 and 1,060 cm<sup>-1</sup>, which are attributed to -OH vibrations and C=O/C-O vibrations. Similar results were reported by Petrović [25]. Therefore, FTIR analysis suggests the aromatic structure of ABC with oxygenic functional groups.

Fig. 1b shows the XRD pattern of ABC. Compared with raw camphor leaf, XRD spectrum of ABC shows loss of peaks at 21.5° and 15.0° assigned to crystalline cellulose [7], indicating the destruction of crystalline structure in the process of biochar preparation. The broad peak around 24.2° indicates the formation of turbostratic carbon crystallites [26]. The SEM image of ABC is shown in Fig. 1c. SEM image of ABC shows uneven surface and porous morphology. Basically, the porous structure of ABC is derived from raw material. Pyrolysis of carbohydrates in raw material generates more pore structure, and KOH activation improves porous structure of biochar via removing organic matter or ash from the surface or pores.

The porous structure provides larger contact surface for Pb(II) adsorption. The specific surface area of ABC was determined by N<sub>2</sub> adsorption-desorption. As shown in Fig. 1d, the isotherm for ABC exhibits a type IV pattern with H3 hysteresis loop according to the IUPAC classification, implying mesoporous characteristics [27]. Table 1 lists the BET, micropore and external surface areas, as well as total, micropore and mesopore volume. The BET surface area ( $S_{\text{BET}}$ ) of ABC is 75.18 m<sup>2</sup> g<sup>-1</sup>. The micropore surface area ( $S_{\text{mi}}$ ) is larger than the external surface area ( $S_{\text{ex}}$ ), and the micropore volume ( $V_{\text{mi}}$ ) is approximately equal to the mesopore volume ( $V_{\text{me}}$ ). This indicates the developed micropore structure, which is attributed to KOH activation. Additionally, the porous structure facilitates Pb(II) diffusion on ABC surface in adsorption process.

### 3.2. Effect of ABC dose

As shown in Fig. 2, Pb(II) adsorption onto ABC soars strictly within 0.04–0.1 g of ABC dose. The Pb(II) removal increases from 41.37% to 99.81% suggesting a strong affinity between ABC and heavy metal, such as lead, which is similar to other report [28]. However, the Pb(II) removal increases slightly when dose of ABC increases from 0.1 to 0.14 g, that may be resulting from the aggregation of many fine particles and the lack of lead ions. Low concentration of heavy metals causes weak concentration-gradient between solution and adsorbent surface. Aggregation of particles decreases the active point on adsorbent surface [29]. Considering the effect of dose of adsorbent on Pb(II) adsorption onto ABC, 0.1 g of ABC is selected as the appropriate dosage of ABC for Pb(II) removal.

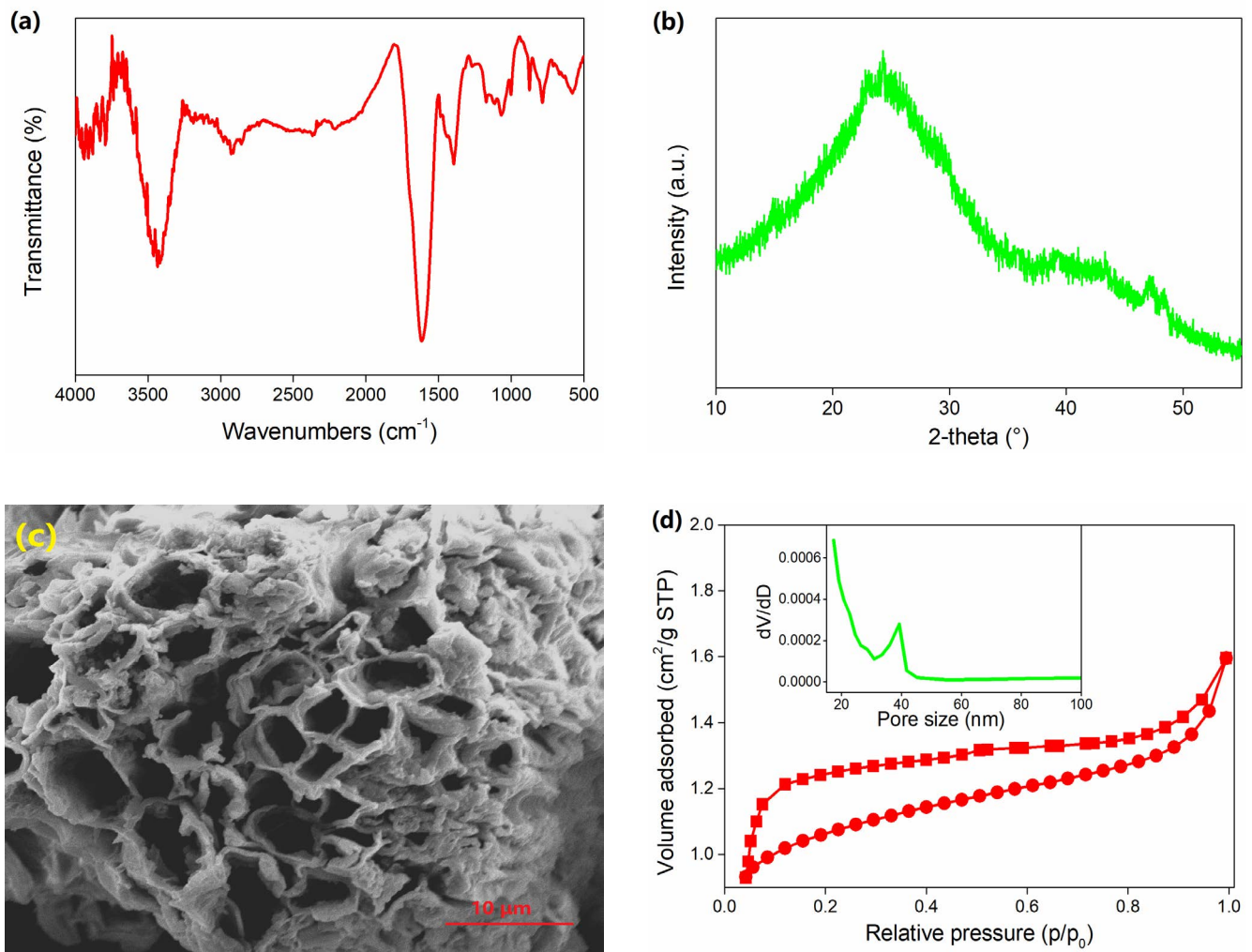


Fig. 1. (a) FTIR spectrum, (b) XRD pattern, (c) SEM image, and (d)  $N_2$  adsorption–desorption of ABC.

Table 1  
Surface texture of ABC

$S_{\text{BET}}$ ( $\text{m}^2 \text{g}^{-1}$ )	75.1819
$S_{\text{mi}}$ ( $\text{m}^2 \text{g}^{-1}$ )	47.8982
$S_{\text{ex}}$ ( $\text{m}^2 \text{g}^{-1}$ )	27.2839
$V_{\text{mi}}$ ( $\text{cm}^3 \text{g}^{-1}$ )	0.0248
$V_{\text{me}}$ ( $\text{cm}^3 \text{g}^{-1}$ )	0.0267
$V_{\text{tot}}$ ( $\text{cm}^3 \text{g}^{-1}$ )	0.0852
Pore size (nm)	29.4396

### 3.3. Effect of pH on Pb(II) adsorption

Solution pH is a key parameter for metal ions adsorption. It influences the activity of surface groups and solution chemistry of metal ions [30]. Based on the study of Jiang et al. [31], the pH range of 1.0–6.0 for Pb(II) adsorption research is reasonable. Insoluble lead hydroxide starts precipitating from the aqueous solution at high concentration (about  $200 \text{ mg L}^{-1}$ ) when pH value is higher than 6.0 ( $K_{\text{spPb(OH)}_2} = 1.42 \times 10^{-20}$ ). In order to avoid the undesirable

deduction of Pb(II), low pH value ( $<6.0$ ) is proper for the research of Pb(II) adsorption [11]. As shown in Fig. 3a, Pb(II) removal and adsorption capacity increase with an increase of pH. At pH below 2.0, ABC shows low efficiency for Pb(II) adsorption. When pH is between 2.0 and 4.0, Pb(II) adsorption is significantly influenced by pH. At pH above 4.0, Pb(II) removal is insensitive to solution pH. These results are attributed to the competitive adsorption between hydrogen ions and Pb(II) ions, as well as protonation of functional groups at acidic condition [7].

The pH value of zero charge ( $\text{pH}_{\text{pzc}}$ ) is the point where the surface acidic functional groups no longer contribute to the pH of the solution. The charge of adsorbent surface will be positive when pH value of solution is lower than  $\text{pH}_{\text{pzc}}$ , further limiting the adsorption of cations. On the contrary, adsorption of cations will be favorable. As shown in Fig. 3b, the pH value of zero charge is about 4.5 based on the measurement of zeta potential, which is similar with reported literature [31]. Adsorption of Pb(II) onto ABC will be favorable due to electrostatic force when pH is higher than 4.5. Associating with the discussion in Fig. 3a, pH value of 6.0 is proper for Pb(II) removal.

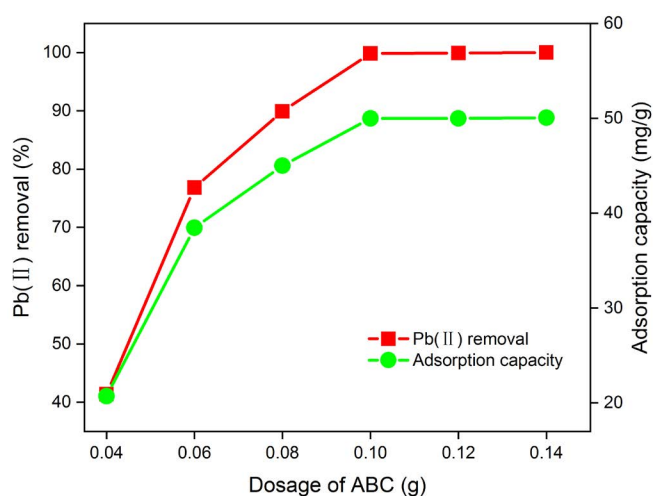


Fig. 2. Effect of dose on Pb(II) adsorption onto ABC (parameters: Pb(II) concentration  $200 \text{ mg L}^{-1}$ , pH 6, temperature  $25^\circ\text{C}$ , adsorption time 30 min).

### 3.4. Effect of ionic strength on Pb(II) adsorption

The effect of Na(I) and Ca(II) concentrations on the removal of Pb(II) by ABC are shown in Fig. 4. It is clear that the removal rate of Pb(II) by ABC decreases gradually with the increase of Na(I) and Ca(II) concentration, and the effect of Ca(II) on the removal of Pb(II) is greater than that of Na(I). This is mainly due to the positive charges of both Na(I) and Ca(II) in the solution, which will affect the interface potential and the thickness of the double layer [32], thus forming a competitive adsorption with Pb(II) and affecting the removal of Pb(II) by ABC. In addition, Ca(II) at the same concentration carries more positive charges than Na(I), so Ca(II) has a greater effect on the removal of Pb(II).

### 3.5. Effect of contact time on Pb(II) adsorption

In Fig. 5b, Pb(II) removal and sorption capacity on ABC increase remarkably within initial 20 min and reach a plateau with an increase of adsorption time. Fast adsorption in

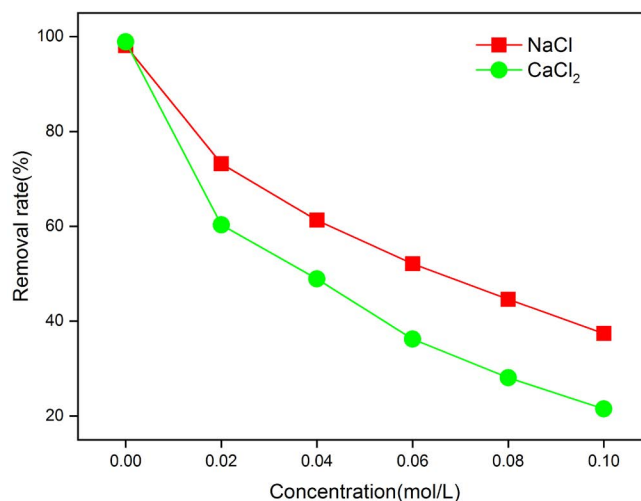


Fig. 4. Effect of ionic strength on Pb(II) adsorption onto ABC (parameters: biochar dosage  $4 \text{ g L}^{-1}$ , Pb(II) concentration  $200 \text{ mg L}^{-1}$ , adsorption time 30 min, pH 6.0, temperature  $25^\circ\text{C}$ ).

initial stage is attributed to rapid external mass transfer and surface adsorption, due to the presence of abundant Pb(II) ions and adsorption sites. The gradual sorption is ascribed to few Pb(II) ions in aqueous solution and nearly saturation adsorption. Pb(II) removal and adsorption capacity is 99.83% and  $50.22 \text{ mg g}^{-1}$  at 30 min, indicating high adsorption rate of Pb(II) onto ABC. This can be attributed to porous structure and large surface area of ABC. As shown in Fig. 5a, it spends 240 min for BC to get roughly the same Pb(II) removal and adsorption capacity as that of ABC. So, biochar has an excellent dynamics performance after activation by cold KOH.

### 3.6. Effect of temperature on Pb(II) adsorption

Temperature is an important factor for Pb(II) adsorption at liquid/solid interfaces. Effect of temperature on Pb(II) adsorption is presented in Fig. 6. As shown in Fig. 6a, Pb(II) removal and adsorption capacity of BC increase about 0.75%

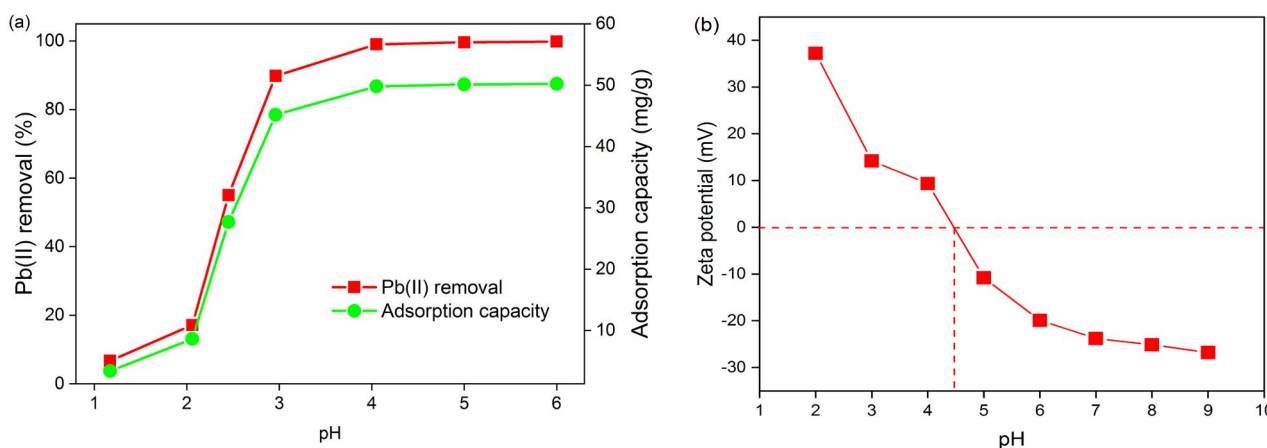


Fig. 3. (a) Effect of pH on Pb(II) adsorption onto ABC (parameters: biochar dosage  $4 \text{ g L}^{-1}$ , Pb(II) concentration  $200 \text{ mg L}^{-1}$ , adsorption time 30 min, temperature  $25^\circ\text{C}$ ) and (b)  $\text{pH}_{\text{pzc}}$  of ABC.

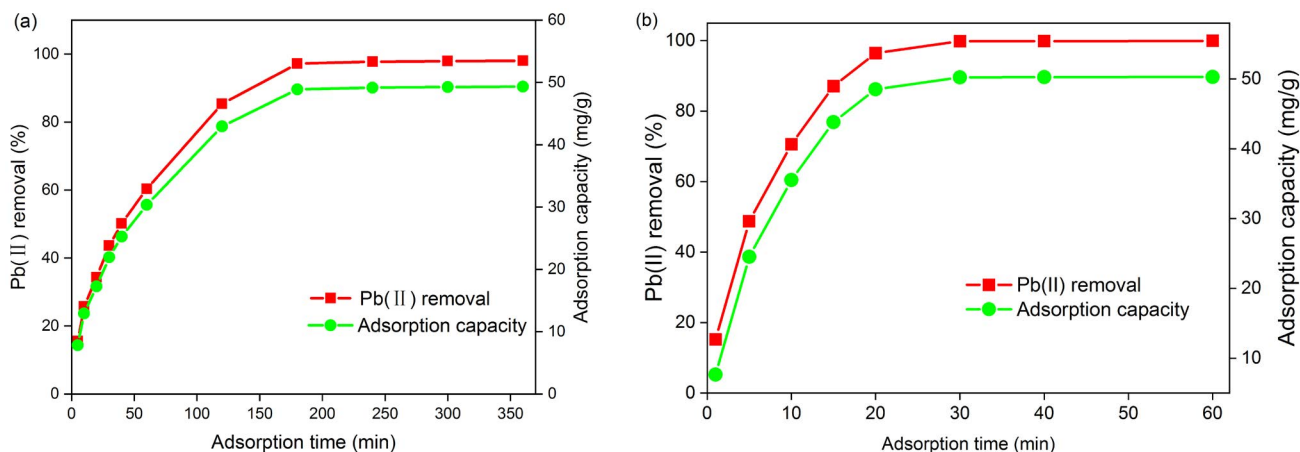


Fig. 5. Effect of contact time on Pb(II) sorption onto (a) BC and (b) ABC (parameters: biochar dosage  $4 \text{ g L}^{-1}$ , Pb(II) concentration  $200 \text{ mg L}^{-1}$ , pH 6.0, temperature  $25^\circ\text{C}$ ).

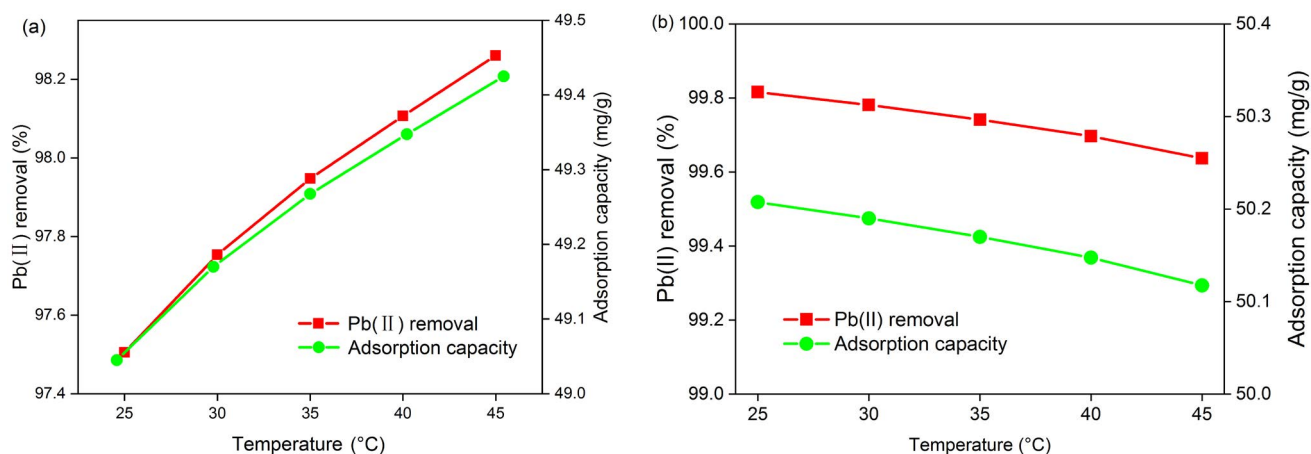


Fig. 6. Effect of temperature on Pb(II) sorption onto (a) BC and (b) ABC (parameters: biochar dosage  $4 \text{ g L}^{-1}$ , Pb(II) concentration  $200 \text{ mg L}^{-1}$ , adsorption time 30 min for ABC and 240 min for BC, pH 6.0).

and  $0.4 \text{ mg g}^{-1}$  respectively, indicating beneficial effect of high temperature on Pb(II) adsorption. Different from Pb(II) adsorption onto BC, Pb(II) removal and adsorption capacity of ABC decreases slightly with increasing temperature (Fig. 6b). When temperature increases from  $25^\circ\text{C}$  to  $45^\circ\text{C}$ , Pb(II) removal decreases from 99.82% to 99.63%, and adsorption capacity decreases from  $50.21$  to  $50.12 \text{ mg g}^{-1}$ . Thus, lower temperature is beneficial for Pb(II) adsorption onto ABC, but the effect of temperature is considerably limited.

### 3.7. Adsorption kinetics

In general, adsorption of metal ions involves three processes: external diffusion, intraparticle diffusion and chemisorption/physisorption [33]. Adsorption kinetics offers insights into adsorption process and reveals the practical applicability of adsorbents. In addition, the kinetics describes the contaminant uptake rate and further, decides residence time of the heavy metals at the solid/solution interface [34]. According to the research of Jiang et al. [31], the pseudo-first-order and pseudo-second-order kinetic models were employed to study the kinetics of Pb(II) adsorption

onto BC and ABC satisfactorily. The results of linear fitting are shown in Fig. 7, and kinetic parameters are listed in Table 2. For both BC and ABC, the correlation coefficient of pseudo-first-order model is considerably less than that of pseudo-second-order model. Also, the calculated value of equilibrium adsorption capacity from pseudo-second-order model agrees with experimental value. This suggests that Pb(II) adsorption onto BC and ABC obeys pseudo-second-order kinetics. Therefore, the rate-limiting step of Pb(II) sorption onto ABC and BC may be chemisorption with exchange or sharing of electrons [35]. However, rate constant of pseudo-second-order model for ABC adsorption is obviously larger than that for BC, indicating an excellent dynamics performance of ABC.

### 3.8. Adsorption isotherms

Adsorption isotherms give important information of adsorption equilibrium. The maximum adsorption capacity provided by adsorption isotherm gives a direct evaluation of the practicability of adsorbents. Two common models, Langmuir and Freundlich isotherms, are

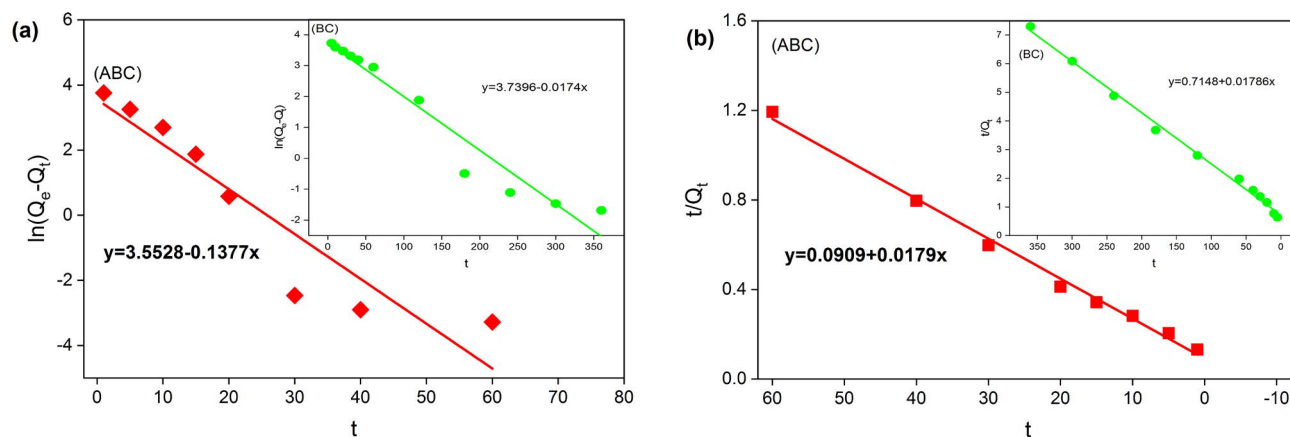


Fig. 7. Linear fitting of (a) pseudo-first-order and (b) pseudo-second-order kinetic models.

Table 2  
Kinetic parameters for Pb(II) sorption

Parameters	Pseudo-first-order model			Pseudo-second-order model		
	$Q_e$ (mg g <sup>-1</sup> )	$k_1$ (min <sup>-1</sup> )	$R^2$	$Q_e$ (mg g <sup>-1</sup> )	$k_2$ (g mg <sup>-1</sup> min <sup>-1</sup> )	$R^2$
ABC	34.9109	0.1377	0.8585	56.0224	0.0035	0.9939
BC	42.0812	0.0174	0.9452	55.9901	0.00045	0.9956

used to examine adsorption equilibrium. Linear fitting of Langmuir and Freundlich models are shown in Fig. 8, and the parameters are listed in Table 3. For Pb(II) sorption onto ABC and BC, the correlation coefficients of Langmuir model are larger than that of Freundlich model. Associated with the agreement of calculated and experimental adsorption capacity, Pb(II) sorption onto ABC and BC is well described by Langmuir model, which is consistent with the research of Cao et al. [36]. Based on Langmuir hypothesis, similar with BC, ABC has homogenous surface and performs monolayer adsorption [37]. The Langmuir parameter  $R_L$ , equaling to  $1/(1 + bC_0)$ , reveals adsorption characteristics: reversible adsorption ( $R_L = 0$ ), favorable adsorption ( $0 < R_L < 1$ ), linear adsorption ( $R_L = 1$ ), and unfavorable adsorption

( $R_L > 1$ ) [38]. Additionally, Freundlich parameter  $n$  suggests well ( $2 < n < 10$ ), difficult ( $1 < n < 2$ ) and poor ( $n < 1$ ) adsorption characteristics [35]. Comparing with the Langmuir and Freundlich parameters of BC, The values of  $R_L$  and  $n$  imply more favorable Pb(II) adsorption onto ABC [11].

Maximum monolayer adsorption capacity of Pb(II) onto ABC for is 90.09 mg g<sup>-1</sup>, higher than 62.27 mg g<sup>-1</sup> of BC. The larger adsorption capacity of Pb(II) onto ABC is owing to large surface area, well-developed micropores and abundant functional groups. As shown in Table 4, the adsorption capacity of Pb(II) onto ABC is comparable with or higher than that of reported biochar or activated carbon. Compared with other modifications or activation processes, cold KOH activation has considerable

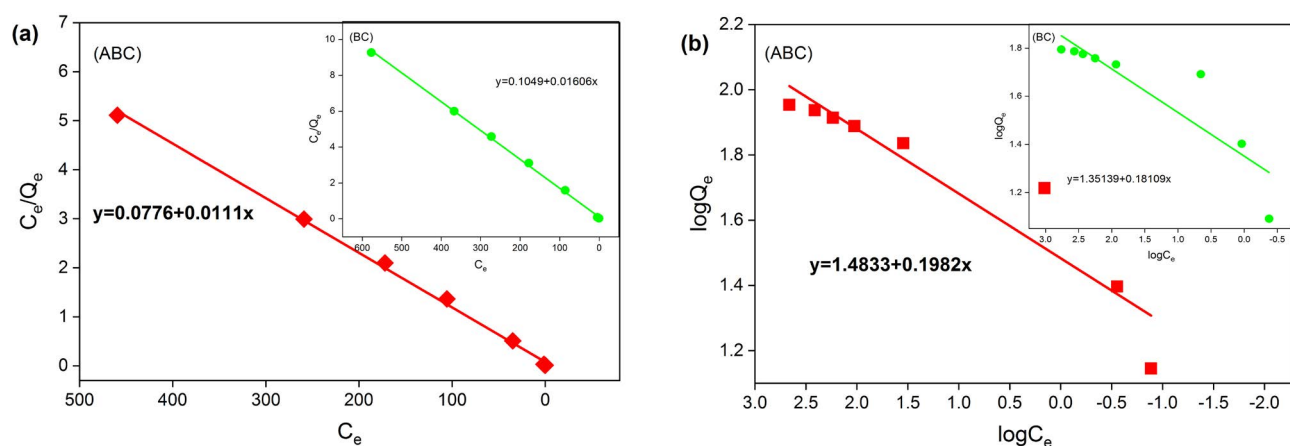


Fig. 8. Linear fitting of (a) Langmuir and (b) Freundlich isotherms.

Table 3  
Isotherm parameters for Pb(II) sorption

Parameters	Langmuir model				Freundlich model		
	$Q_m$ (mg g <sup>-1</sup> )	$b$ (L mg <sup>-1</sup> )	$R_L$	$R^2$	$k_f$ (mg <sup>1-1/n</sup> L <sup>1/n</sup> g <sup>-1</sup> )	$n$	$R^2$
ABC	90.0901	0.1430	0.1155	0.9976	30.4306	5.0454	0.8733
BC	62.2665	0.1531	0.1227	0.9989	22.4589	5.5221	0.7905

Table 4  
Comparison of maximum sorption capacity of Pb(II) onto biochar and activated carbon

Raw materials	Modification	pH	Temperature (°C)	Surface area (m <sup>2</sup> g <sup>-1</sup> )	Adsorption capacity (mg g <sup>-1</sup> )	References
Camphor leaf	Nanoparticles	5.8	30	–	146.84	[19]
Camphor leaf	KOH	6.0	25	75.18	90.09	This study
Rice husk	Nano-MnO <sub>x</sub>	5.0	25	340.0	86.50	[20]
Oak bark	Magnetization	5.0	25	8.8	55.91	[39]
Pine bark	Magnetization	5.0	–	–	25.29	[21]
Pine cone	H <sub>3</sub> PO <sub>4</sub>	5.2	25	1,094.1	27.53	[40]
Coconut shell	H <sub>2</sub> SO <sub>4</sub>	4.5	35	265.96	26.50	[41]

advantages such as low cost, simple operation and high efficiency. Fallen camphor leaves, as local biowastes, is free of charge, eco-friendly and renewable, and thus is promising as raw material of biochar for solving lead pollution in China.

### 3.9. Adsorption thermodynamics

Thermodynamic studies reveal the spontaneity, endothermic or exothermic nature of adsorption process. Linear fitting of  $\ln K_c$  vs.  $1/T$  for Pb(II) adsorption onto ABC and BC is shown in Fig. 9. The calculated thermodynamic parameters are listed in Table 5. The negative  $\Delta G$  values suggest that Pb(II) adsorption onto ABC and BC is spontaneous under the experimental conditions. The increase of  $\Delta G$  with increasing temperature reveals that higher temperature is adverse to Pb(II) adsorption onto ABC. While, the decrease of  $\Delta G$  with increasing temperature for BC adsorption reveals that high temperature is beneficial to Pb(II) removal. The negative  $\Delta H$  value for Pb(II) adsorption reflects that Pb(II) adsorption onto ABC is an exothermic process. Additionally, the negative  $\Delta S$  value indicates a decreased randomness on ABC surface in

adsorption process. On the contrary, positive  $\Delta H$  and  $\Delta S$  for Pb(II) adsorption onto BC suggest that this process is endothermic and adsorption increases randomness on BC surface. So, mild condition (low temperature) of ABC adsorption might be another advantage comparing with BC.

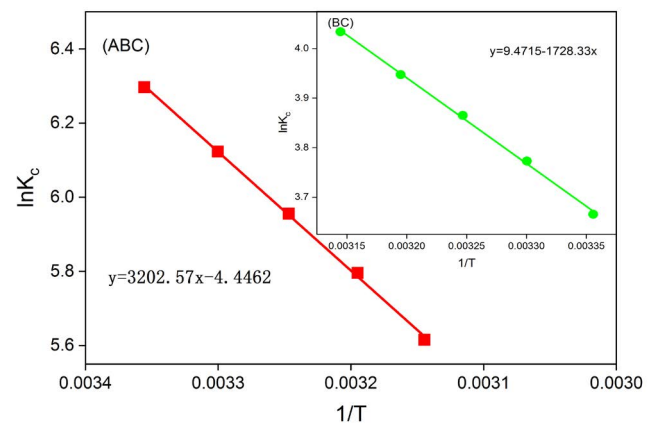


Fig. 9. Linear plot of  $\ln K_c$  vs.  $1/T$  for Pb(II) adsorption.

Table 5  
Thermodynamic parameters for Pb(II) adsorption

Temperature (K)	Thermodynamic parameters		
	$\Delta G$ (kJ mol <sup>-1</sup> , ABC/BC)	$\Delta H$ (kJ mol <sup>-1</sup> , ABC/BC)	$\Delta S$ ((J mol <sup>-1</sup> K <sup>-1</sup> ), ABC/BC)
298	-15.6006/-9.08179		
303	-15.4249/-9.50489		
308	-15.2507/-9.89787	-26.6262/14.3693	-36.9655/78.7461
313	-15.0817/-10.2726		
318	-14.8462/-10.6653		

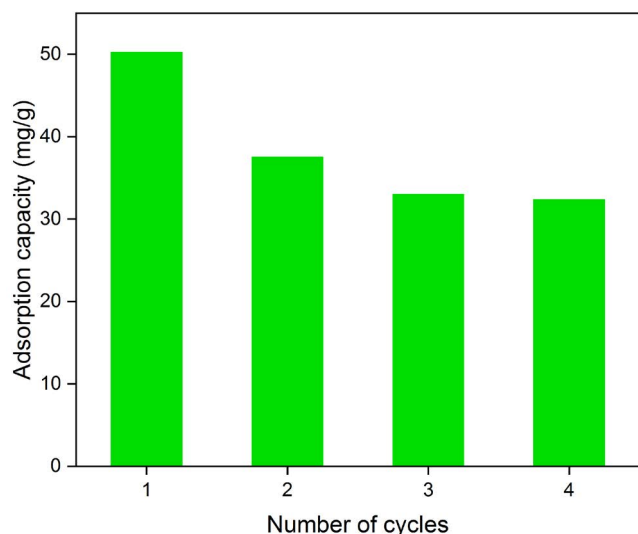


Fig. 10. Regeneration of ABC.

### 3.10. Reusability of adsorbent

The stability of cold KOH activated biochar was researched by the cycles of adsorption/desorption which revealed the reusability of adsorbent. Lasheen et al. [42] reported that hydrochloric acid. As shown in Fig. 10, in the first cycle, adsorption capacity of adsorbent can be  $50.23 \text{ mg g}^{-1}$ . The adsorption capacity slips to about  $30 \text{ mg g}^{-1}$  after four times of adsorption/desorption cycles. Generally speaking, this adsorbent can remove lead ions stably within three or less cycles of adsorption/desorption.

## 4. Conclusions

Biochar (BC) of camphor leaves was activated by cold KOH (ABC) and relative adsorption experiments and characterizations were conducted to research the adsorption performance of ABC. FTIR, XRD, SEM and  $\text{N}_2$  adsorption-desorption reveal that ABC owns oxygen-containing groups, porous structure and large surface area. Pb(II) adsorption onto ABC is highly related to pH, adsorption time and ionic strength while the effect of temperature is limited. Pb(II) adsorption onto ABC is well described by pseudo-second-order kinetics and Langmuir isotherm, implying that Pb(II) adsorption onto ABC is chemisorption and monolayer adsorption and favorable adsorption. The thermodynamics confirms the spontaneous and exothermic nature of Pb(II) adsorption onto ABC. The maximum adsorption capacity of Pb(II) onto ABC is  $90.09 \text{ mg g}^{-1}$ , higher than  $62.27 \text{ mg g}^{-1}$  of BC. ABC can get equilibrium adsorption capacity within 30 min that is much less than the time of BC adsorption, indicating an excellent dynamic performance of ABC. In addition, ABC might get favorable adsorption capacity at lower temperature. Compared with other modifications or activation processes, cold KOH activation has considerable advantages such as low cost, simple operation and high efficiency. Fallen camphor leaves, as local biowastes, is free of charge, eco-friendly and renewable, and thus is promising as raw material of biochar for solving lead pollution in China.

## References

- [1] C.F. Carolin, P.S. Kumar, A. Saravanan, G.J. Joshiba, Mu. Naushad, Efficient techniques for the removal of toxic heavy metals from aquatic environment: a review, *J. Environ. Chem. Eng.*, 5 (2017) 2782–2799.
- [2] P.B. Tchounwou, C.G. Yedjou, A.K. Patlolla, D.J. Sutton, Heavy Metals Toxicity and the Environment, A. Luch, Eds., Molecular, Clinical and Environmental Toxicology, Springer, Basel, 2012, pp. 133–164.
- [3] M.K. Mondal, Removal of Pb(II) ions from aqueous solution using activated tea waste: adsorption on a fixed-bed column, *J. Environ. Manage.*, 90 (2009) 3266–3271.
- [4] B. He, Z.J. Yun, J.B. Shi, G.B. Jiang, Research progress of heavy metal pollution in China: sources, analytical methods, status, and toxicity, *Chin. Sci. Bull.*, 58 (2013) 134–140.
- [5] K. He, S. Wang, J. Zhang, Blood lead levels of children and its trend in China, *Sci. Total. Environ.*, 407 (2009) 3986–3993.
- [6] F.Y. AlJaberi, Investigation of electrocoagulation reactor design effect on the value of total dissolved solids via the treatment of simulated wastewater, *Desal. Wat. Treat.*, 120 (2018) 141–149.
- [7] C. Wang, H. Wang, Y. Liu, Purification of Pb (II) ions from aqueous solution by camphor leaf modified with succinic anhydride, *Colloids Surf., A*, 509 (2016) 80–85.
- [8] H.P. Peng, G.D. Fana, X.M. Zheng, J. Luo, J.J. Zhou, Impact of structure and morphology of titanate nanomaterials on  $\text{Pb}^{2+}$  adsorption in aqueous solution, *Desal. Wat. Treat.*, 136 (2018) 306–319.
- [9] B. Fryczkowska, D. Biniś, C. Ślusarczyk, J. Fabia, J. Janicki, Properties and application of cellulose membranes with graphene oxide addition for removal of heavy metals from aqueous solutions, *Desal. Wat. Treat.*, 132 (2018) 253–262.
- [10] A. Kalra, P. Hadi, H.R. Mackey, T.A. Ansari, G. McKay, Sorption of heavy metal ions onto e-waste-derived ion-exchange material – selecting the optimum isotherm, *Desal. Wat. Treat.*, 126 (2018) 196–207.
- [11] C. Wang, H. Wang, G. Gu, Ultrasound-assisted xanthation of cellulose from lignocellulosic biomass optimized by response surface methodology for Pb(II) sorption, *Carbohydr. Polym.*, 182 (2018) 21–28.
- [12] M.K. Uddin, A review on the adsorption of heavy metals by clay minerals, with special focus on the past decade, *Chem. Eng. J.*, 308 (2017) 438–462.
- [13] J. Lehmann, A handful of carbon, *Nature*, 447 (2007) 143.
- [14] M. Ahmad, A.U. Rajapaksha, J.E. Lim, M. Zhang, N. Bolan, D. Mohan, M. Vithanage, S.S. Lee, Y.S. Ok, Biochar as a sorbent for contaminant management in soil and water: a review, *Chemosphere*, 99 (2014) 19–33.
- [15] J.-H. Park, Y.S. Ok, S.-H. Kim, J.-S. Cho, J.-S. Heo, R.D. Delaune, D.-C. Seo, Competitive adsorption of heavy metals onto sesame straw biochar in aqueous solutions, *Chemosphere*, 142 (2016) 77–83.
- [16] E.B. Son, K.M. Poo, J.S. Chang, K.J. Chae, Heavy metal removal from aqueous solutions using engineered magnetic biochars derived from waste marine macro-algal biomass, *Sci. Total. Environ.*, 615 (2018) 161–168.
- [17] J.-H. Park, J.J. Wang, S.-H. Kim, J.-S. Cho, S.-W. Kang, R.D. Delaune, K.-J. Han, D.-C. Seo, Recycling of rice straw through pyrolysis and its adsorption behaviors for Cu and Zn ions in aqueous solution, *Colloids Surf., A*, 533 (2017) 330–337.
- [18] A.A. Abdelhafez, J. Li, Removal of Pb(II) from aqueous solution by using biochars derived from sugar cane bagasse and orange peel, *J. Taiwan Inst. Chem. Eng.*, 61 (2016) 367–375.
- [19] L. Pi, R. Jiang, W.C. Zhou, H. Zhu, W. Xiao, D.H. Wang, X.H. Mao,  $\text{g-C}_3\text{N}_4$  Modified biochar as an adsorptive and photocatalytic material for decontamination of aqueous organic pollutants, *Appl. Surf. Sci.*, 358 (2015) 231–239.
- [20] C. Wang, H. Wang, Pb(II) sorption from aqueous solution by novel biochar loaded with nano-particles, *Chemosphere*, 192 (2018) 1–4.
- [21] H. Yu, J. Liu, J. Shen, X. Sun, J. Li, L. Wang, Preparation of MnOx-loaded biochar for  $\text{Pb}^{2+}$  removal: adsorption performance and possible mechanism, *J. Taiwan Inst. Chem. Eng.*, 66 (2016) 313–320.

- [22] M.H. Salmani, M. Miri, M.H. Ehrampoush, A. Alahabadi, A. Hosseini-Bandegharai, Comparing cadmium removal efficiency of a magnetized biochar based on orange peel with those of conventional orange peel and unmodified biochar, *Desal. Wat. Treat.*, 82 (2017) 157–169.
- [23] T. Ai, X.J. Jiang, H.M. Yu, H.B. Xu, D.W. Pan, Q.Y. Liu, D.Y. Chen, J.Y. Li, Equilibrium, kinetic and mechanism studies on the biosorption of  $\text{Cu}^{2+}$  and  $\text{Ni}^{2+}$  by sulfur-modified bamboo powder, *Korean J. Chem. Eng.*, 32 (2015) 342–349.
- [24] K. Sun, J. Tang, Y. Gong, H. Zhang, Characterization of potassium hydroxide (KOH) modified hydrochars from different feedstocks for enhanced removal of heavy metals from water, *Environ. Sci. Pollut. Res.*, 22 (2015) 16640–16651.
- [25] J.T. Petrović, M.D. Stojanović, J.V. Milojković, M.S. Petrović, T.G. Šošarić, M.D. Laušević, M.L. Mihajlović, Alkali modified hydrochar of grape pomace as a perspective adsorbent of  $\text{Pb}^{2+}$  from aqueous solution, *J. Environ. Manage.*, 182 (2016) 292–300.
- [26] P. Kim, A. Johnson, C.W. Edmunds, M. Radosevich, F. Vogt, T.G. Rials, N. Labbé, Surface functionality and carbon structures in lignocellulosic-derived biochars produced by fast pyrolysis, *Energy Fuels*, 25 (2011) 4693–4703.
- [27] R.R. Rajagopal, L.S. Aravinda, R. Rajarao, B.R. Bhat, V. Sahajwalla, Activated carbon derived from non-metallic printed circuit board waste for supercapacitor application, *Electrochim. Acta*, 211 (2016) 488–498.
- [28] H. Zheng, J. Qi, R. Jiang, Y. Gao, X. Li, Adsorption of malachite green by magnetic litchi pericarps: a response surface methodology investigation, *J. Environ. Manage.*, 162 (2015) 232–239.
- [29] S. Sun, J. Yang, Y. Li, K. Wang, X. Li, Optimizing adsorption of  $\text{Pb}(\text{II})$  by modified litchi pericarp using the response surface methodology, *Ecotoxicol. Environ. Saf.*, 108 (2014) 29–35.
- [30] K. Vijayaraghavan, Y.S. Yun, Bacterial biosorbents and biosorption, *Biotechnol. Adv.*, 26 (2008) 266–291.
- [31] R.X. Jiang, J.Y. Tian, H. Zheng, J.Q. Qi, S.J. Sun, X.C. Li, A novel magnetic adsorbent based on waste litchi peels for removing  $\text{Pb}(\text{II})$  from aqueous solution, *J. Environ. Manage.*, 155 (2015) 24–30.
- [32] L.J. Dong, W.S. Linghu, D.L. Zhao, Y.Y. Mou, B.W. Hu, A.M. Asiri, K.A. Alamry, D. Xu, J. Wang, Effect of solution chemistry on the removal of  $\text{Co}(\text{II})$  on rice straw-derived biochar, *Desal. Wat. Treat.*, 130 (2018) 161–171.
- [33] N.K. Lazaridis, D.D. Asouhidou, Kinetics of sorptive removal of chromium(VI) from aqueous solutions by calcined  $\text{Mg-Al-CO}_3$  hydrotalcite, *Water Res.*, 37 (2003) 2875–2882.
- [34] Y.M. Pan, R.X. Jiang, J.L. Yang, H. Zheng, E.Q. Yin, Removal of  $\text{Pb}(\text{II})$  ions from aqueous solutions by litchi pericarp and its leachate, *J. Central South Univ.*, 23 (2016) 1626–1632.
- [35] C. Wang, H. Wang, Carboxyl functionalized *Cinnamomum camphora* for removal of heavy metals from synthetic wastewater-contribution to sustainability in agroforestry, *J. Cleaner Prod.*, 184 (2018) 921–928.
- [36] J.S. Cao, R.X. Jiang, J.Q. Wang, J.Y. Sun, Q. Feng, Z.L. Zhao, G.D. Chen, C.R. Zhou, E.Q. Yin, Study on the interaction mechanism between cefradine and *Chlamydomonas reinhardtii* in water solutions under dark condition, *Ecotoxicol. Environ. Saf.*, 159 (2018) 56–62.
- [37] I. Langmuir, The adsorption of gases on plane surfaces of glass, mica and platinum, *J. Am. Chem. Soc.*, 40 (1918) 1361–1403.
- [38] T. Wang, C. Li, C. Wang, H. Wang, Biochar/MnAl-LDH composites for  $\text{Cu}(\text{II})$  removal from aqueous solution, *Colloids Surf., A*, 538 (2018) 443–450.
- [39] D. Mohan, H. Kumar, A. Sarswat, M. Alexandre-Franco, C.U. Pittman Jr., Cadmium and lead remediation using magnetic oak wood and oak bark fast pyrolysis bio-chars, *Chem. Eng. J.*, 236 (2014) 513–528.
- [40] M. Momčilović, M. Purenović, A. Bojić, A. Zarubica, M. Randalović, Removal of lead(II) ions from aqueous solutions by adsorption onto pine cone activated carbon, *Desalination*, 276 (2011) 53–59.
- [41] M. Sekar, V. Sakthi, S. Rengaraj, Kinetics and equilibrium adsorption study of lead (II) onto activated carbon prepared from coconut shell, *J. Colloid Interface Sci.*, 279 (2004) 307–313.
- [42] M.R. Lasheen, N.S. Ammar, H.S. Ibrahim, Adsorption/desorption of  $\text{Cd}(\text{II})$ ,  $\text{Cu}(\text{II})$  and  $\text{Pb}(\text{II})$  using chemically modified orange peel: Equilibrium and kinetic studies, *Solid State Sci.*, 14 (2012) 202–210.